Statistical Mechanics of Ocean Waves

Bruce J. West,* J. Alex Thomson,† and Kenneth M. Watson‡
Physical Dynamics, Inc., Berkeley, Calif.

The evolution of ocean surface spectra due to the nonlinear interaction of surface gravity waves with themselves and ocean currents is discussed. The notions of interacting wave packets (nonlinear waves), incoherence, and nonlinear energy transfer, suggest a general statistical mechanical treatment of the interaction problem. Specific calculations of particular nonlinear interaction mechanisms using an eigenmode analysis are discussed, e.g., the instability of the Stokes' wave and the energy transfer from current patterns to surface waves. Various comparisons with extant ocean and wave tank data are made.

Introduction

THE nonlinear interactions between gravity waves on the surface of the ocean are usually discussed from two distinct points of view. The first is to treat the process as a strictly mechanical interaction between waves. Classically, the approach has been to linearize the dynamic equations to study the interaction, e.g., see Lamb.[1] More recently, however, the nonlinear character of the interaction has been explored. Theoretical analysis has been done by a number of investigators, among whom are Lighthill,[2] Whitham,[3] and West et al.[4] The view has been to construct a set of deterministic, nonlinear equations which can be solved either analytically or numerically on a computer. Experiments have also been conducted to isolate various aspects of the interaction process, e.g., Benjamin and Feir,[5] and others which include the interaction with ocean surface currents, e.g., Lewis et al.[6]

The second viewpoint has been to stress the statistical character of the interaction process and thereby construct a dynamic equation which is applicable to the open ocean environment. Hypotheses, such as the "molecular chaos" assumption of Boltzmann, are employed to randomize the phases of the surface waves[7] to simulate the open ocean environment. This assumption allows one to describe the characteristics of the ocean surface in terms of a spectrum of waves.[8]. Just as in the case of turbulence, this statistical description is in wavenumber space and the theoretical models describe how energy is transferred from one region of the spectrum to another.

The intention of this paper is to present an expression for the dynamic evolution of the inhomogeneous spectral density function which is based on the work of Watson and West.[9] This expression will be used to investigate the effects of surface current gradients on the transfer of energy between spectral regions. These later calculations will include terms modeled in a more heuristic fashion by Thomson and West.[10]

Presented as Paper 74-65 at the AIAA 12th Aerospace Sciences Meeting, Washington, D.C., January 30-February 1, 1974; submitted February 21, 1974; revision received July 22, 1974.

The authors would like to thank B. Cohen, J. C. S. Meng, and A. Davies for development of the computer codes used in this study. This research was supported by the Defense Advanced Research Projects Agency (DARPA), 1400 Wilson Boulevard, Arlington, Va. 22209, and monitored by the Air Force Systems Command, Rome Air Development Center, Griffiss Air Force Base, N. Y. under Contract F30602-C-0494.

Index categories: Oceanography, Physical and Biological; Hydrodynamics; Wave Motion and Sloshing.

*Staff Scientist.

†Vice President and Staff Scientist.

‡Member, Board of Directors and Staff Scientist; also, Professor, Physics Department University of California, Berkeley, Calif.; presently Visiting Professor at Scripps Institute of Oceanography, University of California at San Diego.

Eigenmode Representation

A standard approach to the analysis of the gravity wave interaction problem is to structure the dynamic equations in terms of surface modes. In such a representation, the ocean surface structure is described as a superposition of sinusoidal waves. The clearest example of the utility of this representation is given by a system of linearly-coupled harmonic oscillators. Although each oscillator is completely characterized by its frequency, the coupled system can be excited to a number of different states of oscillation. The frequencies of these states are determined by combining the basis frequencies in different ways. These states are the normal or characteristic modes of the coupled system. Analytically, the existence of these states implies there exists a matrix which will transform the initially-coupled system to one which is uncoupled. This uncoupled state of motion is described by the eigenfunctions of the system.

Nonlinear systems may be simplified using this concept by expressing the nonlinear equations in terms of the linear eigenfunctions. Following Ref. 4, consider the column matrix

$$\boldsymbol{\Psi}(x,t) = (\Psi_1, \Psi_2, \ldots, \Psi_N)$$

which satisfies the differential equation

$$\left(i\frac{\partial}{\partial t} - \mathbf{H}\right)\boldsymbol{\Psi} = \mathbf{F}(\boldsymbol{\Psi}) \tag{1}$$

Here we suppose $\mathbf{H}$ to be a linear Hermitian operator and $\mathbf{F}$ to be a nonlinear function of $\boldsymbol{\Psi}$. If a complete set of eigenfunctions $\chi_k(\mathbf{x})$ of $\mathbf{H}$ exist, with eigenvalues ω_k

$$\mathbf{H}\,\chi_k = \omega_k \chi_k \tag{2}$$

we may expand ψ in the form

$$\boldsymbol{\Psi} = \sum_k B(k)\chi_k(x)e^{-i\omega_k t} \tag{3}$$

Forming the scalar product of both sides of Eq. (1) with χ_k^* leads to a set of coupled first-order equations for the B's.

The eigenmode equations describing the interaction of surface gravity waves, including a surface current U which has the harmonic decomposition

$$U = \sum_K U_K \cos K\xi; \quad \xi = x - c_0 t \tag{4}$$

is[11]

$$\begin{aligned} i\dot{B}^{(\pm)}(k) &= (\omega_k - k_x c_0)B^{(\pm)}(k) \\ &+ \frac{1}{4}\sum_K k\cdot U_K[B^{(\pm)}(k-K) + B^{(\pm)}(k+K)] \\ &+ \sum_{\substack{\ell+p=k \\ s_1,s_2}} \Gamma^k_{\ell,p} B^{(s_1)}_{(\ell)} B^{(s_2)}_{(p)} + \sum_{\substack{\ell+p=k+n \\ s_1,s_2,s_3}} \Gamma^{kn}_{\ell p} B^{(s_1)}_{(\ell)} B^{(s_2)}_{(p)} B^{(s_3)}_{(n)} \\ &+ \ldots \end{aligned} \tag{5}$$

Equation (5) describes the coupling between modes for an inviscid, incompressible, irrotational ocean in the absence of wind. The quantities $B^{(\pm)}$ $(\boldsymbol{k})$ are the mode amplitudes for right (+) and left(−) propagating waves as distinguished by $s_i = \pm$, $i = 1, 2, \ldots$, in the summations.

The first term in Eq. (5) gives the phase shift of the $\boldsymbol{k}$ mode due to the presence of the translating current with k_x as the x component of the surface wavenumber and c_0 the phase velocity of the current pattern. If the surface current is written as a harmonic series as in Eq. (4), the second term gives the coupling to the surface waves. Note that $\boldsymbol{k}$ is coupled to $\boldsymbol{k} \pm \boldsymbol{K}$ by the current, i.e., discrete mode coupling. The remaining two terms give the quadratic and cubic nonlinearities arising from an expansion of Bernoulli's equation and the kinematic boundary condition about the unperturbed ocean surface.

Theorems concerning mode coupling, as well as available examples, imply that for weak coupling, as in the gravity wave case, significant mode coupling occurs only through resonant terms.[4,7] Resonance in Eq. (5) is defined by the expression

$$|\,\omega_k - \sum_{\mathfrak{L}} S_{\mathfrak{L}} \omega_{\mathfrak{L}}\,| \approx 0; \qquad S_{\mathfrak{L}} = \pm 1 \tag{6}$$

along with the restrictions on the sums over $\boldsymbol{k}$,and $\omega_k = (gk)^{1/2}$ is the linear dispersion relation. Since the second-order terms in Eq. (5) cannot both satisfy Eq. (6) and the restriction on wavenumber given in the summation, this term does not contribute significantly to the growth of a mode and may be deleted from the expression.

Modal Experiments

The nonlinear part of the gravity wave interaction takes the form of mode coupling or mixing as represented in Eq. (5). Mode mixing of deep water waves was first demonstrated in a tank experiment by Benjamin and Feir.[5] A train of sinusoidal waves mechanically generated at one end of a tank lost their periodic structure and appeared randomized at some distance from the source. A linear stability calculation made by Benjamin and Feir showed that wave instability occurs with the development of sidebands of a finite amplitude sinusoidal wave. A simulation of this experiment using Eq. (5) was conducted using 13 modes and is shown in Fig. 1. The mechanically-generated wave is given by the central mode amplitude, and the twelve other modes in the system are depicted as containing noise with amplitudes two orders of magnitude lower than the central. The sidebands which were determined by linear analysis to be preferentially amplified from out of the background noise are modes one and thirteen. We see that the nonlinear calculation extends the linear notion of a preferred mode to that of a preferred group of modes concentrated in the region given by the linear theory.[4]

This result assists one in resolving some conceptual difficulties which arise when a spectrum is used to describe a nonlinear process such as present at the ocean surface. An example of this difficulty is provided by a Stokes Wave. The exact solution to Bernoulli's equation at the ocean surface for the surface displacement (ζ) is given by the implicit expression

$$\zeta(\xi) = \beta e^{k\zeta(\xi)} \cos k\xi \tag{7}$$

where $\xi = x - c_o t$ is a tranlating coordinate. An explicit series expansion in terms of harmonics of the fundamental wavenumber k is given in a number of places.[12] The amplitudes of the harmonics define a spectrum for the nonlinear Stokes Wave. Because the ocean wave field is dispersive, waves of different wavelength travel at different phase velocities (c), i.e., $c = \omega_k / k$. However, the coupling of the harmonics in the Stokes Wave "freezes" the phase velocities of the different modes so that they are all equal to that of the fundamental. This mode locking gives rise to the persistent shape of the

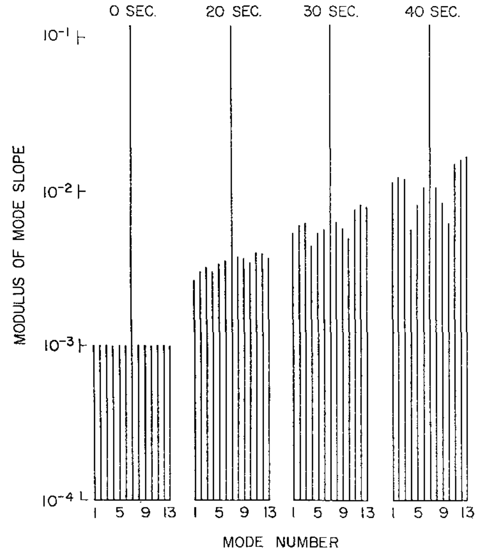

Fig. 1 A thirteen mode simulation of the Benjamin-Feir experiment is depicted. The spectrum is shown at four different times as it evolves by integrating Eq. (5).

Stokes wave which one obtains from Eq. (7). If these phase velocities were not equal, one would observe the wave form to break up. This phase locking gives the impression that the nonlinear interaction between the harmonics is strong. If this coherent effect is present on the ocean, a spectral representation is inappropriate, i.e., phase information is important.

If we write the amplitude of an initially monocromatic wave at the ocean surface as

$$\zeta(x,t) = G(x,t)\zeta(x,o) \tag{8}$$

the function $G(x,t)$ is the envelope function of the fundamental surface wave given by the surface height at time $t=0$, i.e., $\zeta(x,0)$. The simulation of the Benjamin-Feir experiment in terms of $G(x,t)$ is depicted in Fig. 2a. Initially, the modulation of the fundamental wave ($|G|$) is close to zero, but the snapshots of the envelope at times 20 and 30 sec indicate a strong modulation or breakup of the mechanical wave. The Stokes wave is therefore unstable and loses its integrity as it propagates down a tank. The interaction which produces this effect is found to be local in k space and to dominate over the coupling between the wave harmonics. The degree of modulation may be measured by the deviation of the envelope function from its average value as is depicted in Fig. 2b. The surface distortion, as this deviation is called, is near 20% at 30 sec and grows rapidly after this time in agreement with the experimental results.

A second experiment done by Lewis et al.[6] stimulated energy transfer between modes by means of a surface current. In this experiment, an internal wave was generated at a fluid interface near the bottom of a tank. An infinitesimal surface wave was mechanically generated and the modulation of the surface height and slope recorded. This experiment was simulated using the resonant form of Eq. (5) with a single internal wave present.[11]

The linear analysis for this problem has been done by a number of investigators.[6,13] In Figure 3 is indicated the results of our calculation in terms of the surface distortion which is a precise representation of the degree of nonlinear growth. The initial surface wave is infinitesimal, so the cubic terms in the interaction equation do not contribute significantly to the growth of the mode slope. The group velocity of the mechanical wave is equal to the phase velocity of the current, so that a given segment of the surface wave interacts continuously with a given phase point of the internal wave as they both propagate down the tank. The length of time of the in-

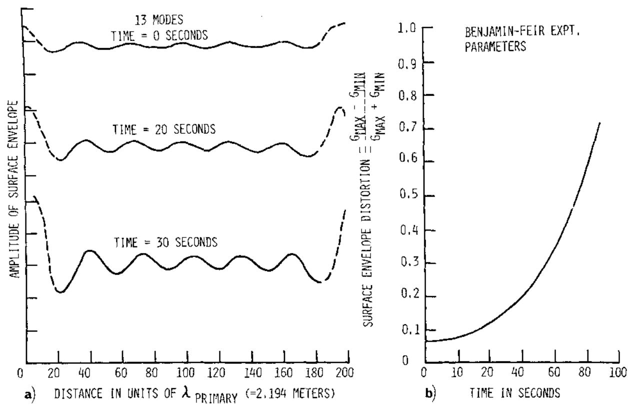

Fig. 2 a) The envelope function for the Benjamin-Feir experiment is depicted at three times.... b) The deviation of the envelope function from the average is shown as a function of time.

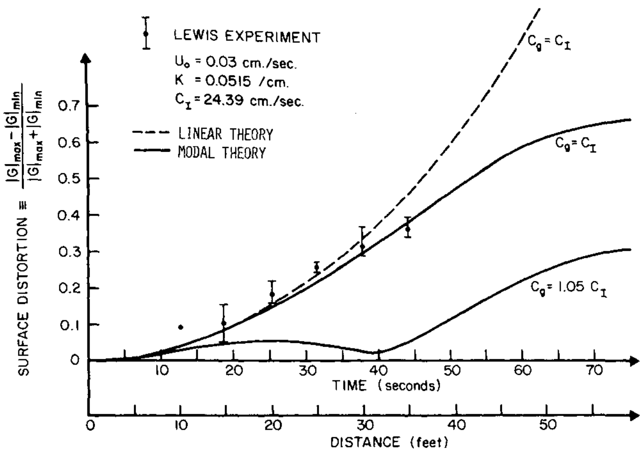

Fig. 3 The surface distortion for the Lewis tank experiment (I) is plotted and compared with three calculations, Two calculations are at resonance $c_g = c_I$, (i) linear (---), (ii) modal (——), and the third calculation is modal theory but not at resonance, i.e., $c_g \neq c_I$.

teraction can therefore be measured as a function of distance down the tank. The linear theory (dashed curve in Fig. 3) agrees with the numerical calculation for a surprisingly long time. The parameters for the experiment indicate that the linear theory will be adequate for interaction times smaller than 50 sec. The sensitivity of the surface distortion to the velocity matching is clear from the surface distortion for a surface wave whose group velocity is 5% "off" resonance, also shown in Fig. 3.

The type of problems most amenable to the eigenmode approach in its present form are those which involve a rather narrow spectral interval. The ocean spectrum, however, spans five decades in wavenumber space. One way to extend our calculation to the extremes of the spectrum and maintain an efficient calculational algorithm is to employ the Fast Fourier Transform technique to evaluate the summations in Eq. (5). A second approach and the one discussed here is to suppress some of the information contained in Eq. (5) as being irrelevant to the description of the ocean surface. To do this systematically, a number of assumptions about the character of the ocean spectrum are made which are consistent with the eigenmode calculations discussed. These assumptions form the statistical hypothesis made in the following sections.

Spectral Transfer Equation

To describe the ocean surface, as opposed to a tank surface, we construct from the mode amplitudes in the preceding section a spectral density function. This function is the Fourier Transform of the variance of the surface displacement and is obtained by making a statistical assumption about the Fourier amplitudes of the surface displacement. To construct the spectral density function, we introduce the amplitude

$$a(\mathbf{k},t) = B(\mathbf{k},t)/|\mathbf{k}|2^{1/2} \tag{9}$$

such that

$$Z(\mathbf{x},t) = \sum_{\mathbf{k}} a(\mathbf{k},t)e^{i\mathbf{k}\cdot\mathbf{x}}$$

and the surface displacement is

$$\zeta(\mathbf{x},t) = \frac{i}{2}\left[Z(\mathbf{x},t) - Z^*(\mathbf{x},t)\right]$$

At some initial time (t_0) the amplitude $a(\mathbf{k},t_0)$ is observed to have the value $a_{\mathbf{k}}$. A series of such measurements conducted at time intervals long compared with the correlation time the $a_{\mathbf{k}}$'s will lead to an ensemble of values for the $a_{\mathbf{k}}$'s. If we denote an ensemble average by the brackets $\langle \ \ldots \ \rangle$ the energy per unit area on the ocean surface is

$$\text{energy/unit area} = \frac{1}{2}\rho g \sum_{\mathbf{k}} \langle |a_{\mathbf{k}}|^2 \rangle \tag{10}$$

If the fluctuations in each $a_{\mathbf{k}}$ are uncorrelated with the fluctuation in any other amplitude, then

$$\langle a_{\mathbf{k}} \rangle = \langle a_{\mathbf{k}} a_{\mathcal{L}} \rangle = 0 \tag{11a}$$

and for a completely incoherent spectrum

$$\langle a_{\mathbf{k}} a^*_{\mathcal{L}} \rangle = \langle |a_{\mathbf{k}}|^2 \rangle \, \delta_{\mathbf{k}\mathcal{L}} \tag{11b}$$

If, however, there is a correlation between the $a_{\mathbf{k}}$'s, we introduce a coherence distance λ such that

$$\langle a_{\mathbf{k}} a^*_{\mathcal{L}} \rangle \neq 0 \quad \text{only if} \quad \mathbf{k} - \lambda/2 \leq \mathcal{L} \leq \mathbf{k} + \lambda/2 \tag{12}$$

i.e., $\mathcal{L}$ must be in the coherence range of the wave vector $\mathbf{k}$. Using this assumption, we partition the surface wave spectrum into M coherence intervals of width $|\lambda|$ and define the quantity

$$F(\mathbf{k},\mathbf{r}) = \frac{1}{2}\rho g \sum_{\Delta} \langle a(\mathbf{k}+\Delta/2) a^*(\mathbf{k}-\Delta/2) \rangle \exp[i\Delta\cdot\mathbf{r}] \tag{13}$$

where Δ is in the coherence intervalλ about $\mathbf{k}$. Equation (13) may be integrated to give the expression

$$\text{total energy/unit area} = \frac{1}{(2\pi)^2} \int\int d^2k d^2r \, F(k,r) \tag{14}$$

Equation (14) implies that $F(\mathbf{k},\mathbf{r})$ is the inhomogeneous spectral density function for the ocean surface and agrees with more traditional definitions, e.g., as given by Phillips,[14] for $\mathbf{r} = 0$. A more complete description of this function is given in Watson and West.[9]

To obtain the equation of evolution for the spectral density function, we use

$$\frac{\partial F(\mathbf{k},\mathbf{r})}{\partial t} = (1/2)\rho g \sum_{\Delta} [\langle \dot{a}(\mathbf{k}+\Delta/2)\, a^*(\mathbf{k}-\Delta/2) \rangle + \langle a(\mathbf{k}+\Delta/2)\, \dot{a}^*(\mathbf{k}-\Delta/2) \rangle] \exp[i\Delta\cdot\mathbf{r}] \tag{15}$$

where the time derivatives on the right-hand side of Eq. (15) are given by

$$\dot{a}(\mathbf{k})+i\omega_k a(\mathbf{k})=\alpha(k)a(\mathbf{k})-\frac{i}{2}\mathbf{k}\cdot\sum_{\mathbf{k}}\mathbf{U}_{\mathbf{K}}\{a(\mathbf{k}-\mathbf{K})+a(\mathbf{k}+\mathbf{K})\}+i\sum_{\pounds+p=k+n}\frac{\pounds pn}{k}\Gamma^{kn}_{\pounds p}\,a(\pounds)\,a(p)\,a^*(n) \tag{16}$$

The function $\alpha(k)$ represents the difference between energy being pumped into a region λ about k by the wind and energy being dissipated in that region, e.g., by viscosity. For this discussion, we leave this function unspecified. For the term coupling the surface waves to the current, we have used $|k| \gg |K|$ to obtain the coupling coefficients from Eq. (5).

The resulting equation of evolution, when Eq. (16) is substituted in Eq. (15), has the schematic form

$$\{\frac{\partial}{\partial t}+\frac{d\mathbf{r}}{dt}\cdot\nabla_{\mathbf{r}}+\frac{d\mathbf{k}}{dt}\cdot\nabla_{\mathbf{k}}\}F(\mathbf{k},\mathbf{r})=\epsilon(\mathbf{k})F(\mathbf{k},\mathbf{r}) \tag{17}$$

where

$$\frac{d\mathbf{r}}{dt}=\nabla_{\mathbf{k}}H;\quad \frac{d\mathbf{k}}{dt}=-\nabla_{r}H \tag{18}$$

For a general surface current U

$$H=k\cdot U+\omega_k-\sum_{\mathbf{L}}D(L,k)F(L,r) \tag{19}$$

and

$$\epsilon(k)=\alpha(k)-\nabla_{\mathbf{r}}\cdot[\frac{kk{:}U}{2k^2}+\sum_{L}\{D_1(L,k)+D_2(L,k)\}F(L,r)] \tag{20}$$

We see that the velocity of a wavepacket [Eq. (18)] has been changed from that expected in linear theory to include the interaction with all other packets present at position $\mathbf{r}$. The function $\mathbf{D}_1(\mathbf{L},\mathbf{k})$ is the $\mathbf{k}$ gradient of the interaction function

$$D(\mathbf{L},\mathbf{k})\equiv\frac{4}{\rho g}L^2\,\Gamma^{\mathbf{kL}}_{\mathbf{kL}} \tag{21}$$

and $\mathbf{D}_2(\mathbf{L},\mathbf{k})$ is the $\mathbf{L}$ gradient. The refraction rate of the wave vector of the packet [Eq. (18)] is also changed from its linear form to include a dependence on the local gradient of the surface spectrum. Finally, the rate at which energy is being supplied to the spectral interval $(\mathbf{k},\ \mathbf{k}+\mathbf{dk})$ is dependent on the product of the local spatial gradient of the surface spectrum and the gradient of the interaction function. This is a modification of Longuet-Higgins and Stewart's 'radiation stress' term[15] associated with the interaction of waves $\mathbf{k}$ with the entire spectrum. Note that these nonlinear terms arise from the coupling terms in Eq. (16).

It is worth stressing that Eq. (17) is the disguised form of an integral equation which is gradratic in the spectral function $F(\mathbf{k},\mathbf{r})$ and is analogous to the Boltzmann equation in Kinetic Theory. It should also be stressed that the modifications in group velocity, refraction rate, and energy transfer rate are not included in previous similar formal treatments of this problem. These effects are included parametrically in the phenomenological treatment of this problem[10] where particular interactive mechanisms are modeled and then appended to the equation of evolution. Hasselmann's treatment[7] of this problem results in an integral expression which is third-order in $F(\mathbf{k},\mathbf{r})$, which is also obtained by keeping terms to fifth-order in the interaction equation [Eq. (5)]. The effect of these higher order terms can, therefore, be added directly to Eq. (17).

Spectral Calculations

The transfer equation describes how energy is fed into ocean waves, how it gets distributed among these waves, and how it is dissipated. The interactive mechanisms included in Eq. (17) are: a) generation of waves by wind, b) linear interaction of the surface spectrum with a current, c) nonlinear wave-wave interactions and d) viscous dissipation of energy. In an empirical formulation of this equation, nonlinear amplitude and capillary effects on group velocity are included, as well as energy dissipation due to breaking waves.

Pierson and Stacy[16] (PS) synthesize experimental data on the development of surface waves as a function of wind friction velocity (U_*). The approach they use is to partition the wavenumber spectrum into five distinct regions, as shown in Fig. 4, and to fit the data by an appropriate spectral function in each of these regions. Figure 4 depicts the surface slope spectrum (k^3F) so obtained as a function of wavenumber k for a wind friction velocity of 24 cm/sec.

In Fig. 5, a numerical integration of the phenomenological transfer equation[10] is compared with the PS spectrum for two values of the viscosity coefficient υ_T. We see that the low wavenumber ($k \leq 0.01$) part of the spectrum is modeled equivalently by PS or the transfer equation for a U_* of 24 cm/sec. The gravity wave-gravity wave equilibrium range essentially rises to a constant value where the PS spectrum becomes the saturated spectrum of Phillips. The transfer equation, however, deviates from the horizontal giving some slope to this region - the angle of which is dependent on U_*. The saturation is therefore enhanced above the value given by *PS*. The transfer equation rises slowly through the connecting regions and is suppressed below the PS spectrum at the start of the capillary range. If the value of the viscosity coefficient (υ_T) is taken to be that of molecular viscosity (υ_{mole}), the transfer spectrum over-emphasizes the capillary regime. This growth represents the sensitive balance between the energy input of the wind and energy dissipation due to viscous damping. With modified values of the viscosity coefficient ($1.7\upsilon_{\text{mole}}$ and $2.5\upsilon_{\text{mole}}$), the spectrum is bounded in the capillary region. It is clear, however, that the capillary region is not saturated.

The transfer equation [Eq. (17)] describes the interactive and transfer mechanisms present at the ocean surface. Additional processess, such as wave breaking and turbulent viscosity, are only partially understood and are included in the transfer equation in a more heuristic manner.[10] The overall agreement with the PS spectrum indicates that the general structure of the transfer equation is appropriate for the infinite fetch case. Application of the transfer equation to more complex cases will be made in the following sections.

Interactions with Surface Currents

The transfer equation in the presence of a temporally-steady but spatially variable current $U(\xi)$ may be integrated along the trajectories defined by Eq. (18). The trajectories of surface wave packets are expressed in dimensionless form by the equations

$$\begin{aligned} d\xi/d\tau &= A(\kappa)/2\kappa^{1/2}+u(\xi) \\ d\kappa/d\tau &= -\kappa[du(\xi)/d\xi] \end{aligned} \tag{22}$$

where $A(\kappa)$ is he group velocity of a surface wave packet of wavenumber $k=g\kappa/U_*^2$ and $u(\xi)$ is the surface current at position $\xi=(x-c_0t)g/U_*^2$, including the effect of wind drift

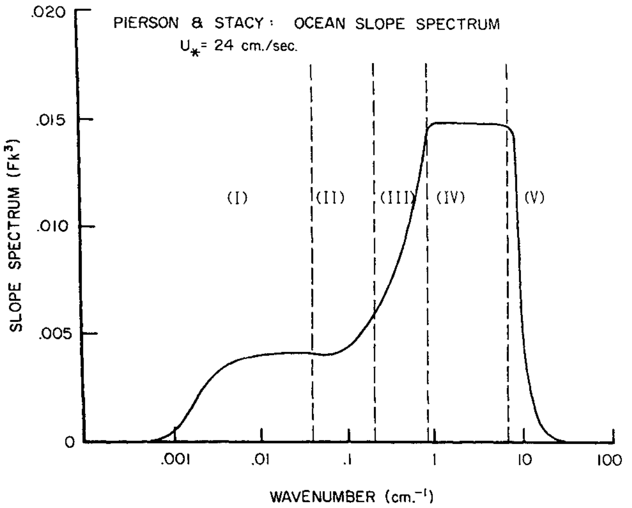

Fig. 4 The fully developed ocean slope spectrum (k^3F) (infinite fetch) as given by the Pierson and Stacey functional fit to data for a wind friction velocity of 24 cm/sec is shown. The five regions of the spectrum are (i) gravity wave—gravity wave equilibrium range, (ii) the isotropic turbulence range, (iii) connecting range of Leykin and Rosenberg, (iv) capillary range, and (v) viscous cutoff range.

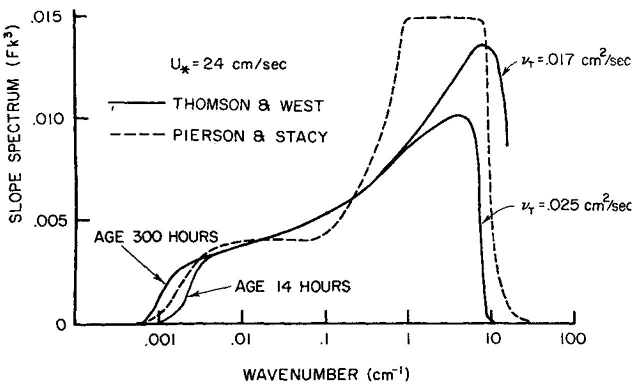

Fig. 5 A comparison of the slope spectrum obtained from a numerical integration of the transfer equation with the Pierson-Stacey spectrum of Fig. 4 is depicted. The dependence on time for the development of long waves and the viscosity coefficient for the dissipation of capillary waves is indicated.

and c_o is the translational velocity of the current pattern.[10] The distance and time scaling parameters are U_*^2/g and U_*/g, respectively.

In Fig. 6a, a Gaussian current pattern is depicted which is translating opposite to the direction of the wind and is given by

$$U(\xi) = -\{1.04 + 0.04 \exp[-\xi^2/\Delta^2]\} \tag{23}$$

in dimensionless form. The pattern translates at 48 cm/sec with a 4% current variation. In the absence of local wave-wave interactions, the trajectories defined by Eq. (22) are depicted in Fig. (6b). A wavepacket launched at a position ξ with a wavenumber κ travels in the direction of the arrows. Wavepackets whose group velocities are close to the translating velocity of the current pattern are reflected in the traveling coordinate system. For the specified current pattern, those wavenumbers which experience reflection are indicated by the bracket labeled resonance region. A complete discussion of this phenomenon is presented in Ref. 17.

The value of the normalized spectrum $Y(\equiv k^3F)$ along these trajectories is obtained by integrating the transfer equation in the form

$$dY/d\tau = G(Y,\kappa,\xi)$$

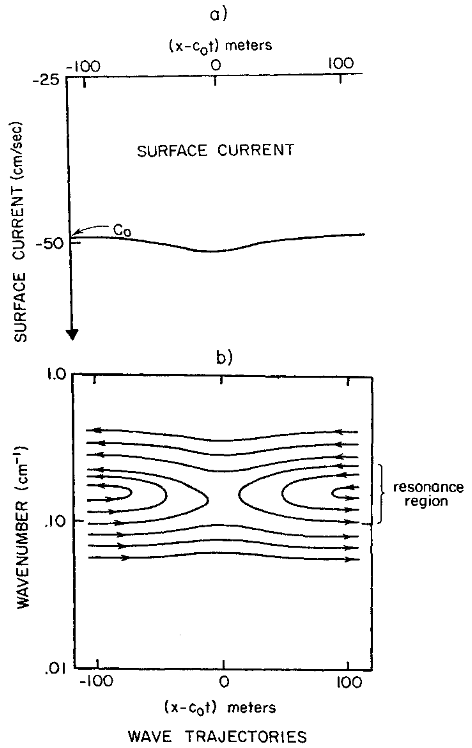

Fig. 6 A variable current, translating with a velocity c_0 is indicated in a). The wave trajectories for the surface waves in the presence of this variable current are indicated in b) in the translating coordinate system $\xi = x - c_0t$.

with

$$\frac{dY}{d\tau} = \frac{\partial Y}{\partial \tau} + \frac{d\xi}{d\tau}\frac{\partial Y}{\partial \xi} + \frac{d\kappa}{d\tau}\frac{\partial Y}{\partial \kappa}$$

and $d\xi/d\tau$ and $d\kappa/d\tau$ are the trajectories given by Eq. (22).

This calculation may be used to indicate the importance of the nonlinear interactions in determining the spectral perturbation produced by the current. The trajectories in Fig. 6b indicate the scattering of the surface waves from the prescribed current pattern in a coordinate system in which the current is temporally steady. The linear calculation of the interaction of the surface waves with the current pattern is affected by "turning off" the finite amplitude effects, the capillary waves, wave-breaking effects, wind and viscosity in the transfer equation. The resulting expression is the spectral transfer equation for infinitesimal surface gravity waves coupled to an adverse ("Gaussian") current.

In Fig. 7, the slope spectrum (k^3F) is graphed vs the log of the wavenumber at four different space points relative to the translating current packet, i.e., the stations are translating with the velocity of the current profile. Because we are in the gravity wave region of the spectrum, the slope spectrum would be a flat horizontal line in the absence of the current, as was discussed with regard to the PS spectrum. The deviation from the horizontal is the spectral perturbation produced by the adverse current. The magnitude of the perturbation on the saturated spectrum, i.e., about an order of magnitude, is in essential agreement with the linear calculation of Ref. 17. In the region upstream of the current ($\xi < 0$), wavelengths shorter than the resonant wavelength are enhanced. In the region downstream of the current ($\xi > 0$), there is a general suppression of the spectrum. Above the current crest, both effects are apparant. This would correspond to a roughening of the surface in advance of the current pattern and a calming behind the pattern. When the same calculation is applied to a fully-developed sea with all the nonlinear terms included, the resonant effect shown in Fig. 7 is strongly suppressed

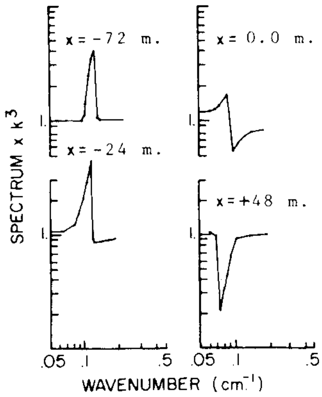

Fig. 7 The perturbation of the surface wave spectrum induced by current pattern in Fig. 6a is depicted at four stationary positions relative to the translating current.

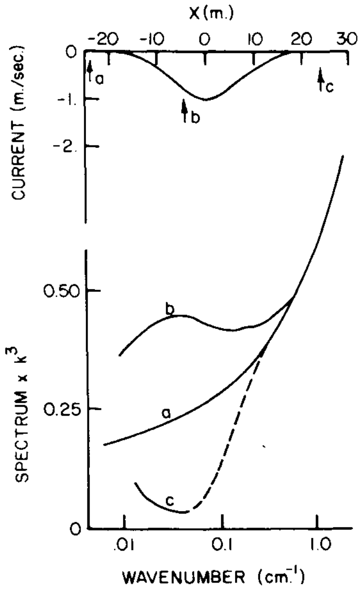

Fig. 8 A variable current, stationary in space, is indicated in a). The perturbation of the surface wave spectrum induced by the current is shown in b) at the three points in space labeled a, b and c in a).

(calculated enhancements at the resonant wavelengths are less than 1% for winds exceeding 10 knots) and significant effects occur only in relatively-stong currents.

In Fig. 8, we show the spectral alternations created when a fully-developed sea driven by a 25-knot wind impinges on a region of adverse current having a peak current of -1.0 m/sec and a half width of about 17 meters. The incident waves are assumed to have reached a balance with the wind input and to have an equilibrium spectrum (spectrum **a** in Fig. 8). Over the region of maximum current, the wave amplitudes are appreciably enhanced (spectrum **b**). However, the resultant increased wave dissipation in this region results in a strong suppression of waves having wavelengths between 6 and 60 cm (spectrum **c**) downwind of the strong current region. The artificial construction of such adverse currents might serve as wavebreakers to shelter harbors, ocean drilling platforms, etc.

The trajectories for the breakwater calculation are depicted in Fig. 9. The trajectories for the fully developed sea impinge on the stationary current pattern from the left. The long, fast gravity waves are perturbed in the region of the current, but return to their ambient wavelengths after passing through the pattern. The shorter waves are distorted more and more by the current, until they gain sufficient speed to get through the

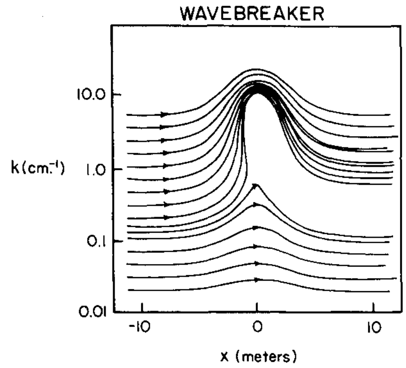

Fig. 9 The wave trajectories for a fully developoed sea in the presence of the stationary current in Fig. 8a are shown.

pattern. These waves, instead of being reflected, as they were in the case of the translating current pattern just discussed, refract to higher and higher wave-numbers. Eventually these compressed waves enter the capillary regime and therefore have a different dispersion relation, i.e., $\omega_k = (gk+\gamma k^3)^{1/2}$, where γ is the kinematic surface tension 72 cm^3/sec^2. The new dispersion relation gives the wave packets sufficient speed, i.e., $c_g = d\omega_k/dk$, to "push" through the breakwater, but at a much higher wavenumber, during which process the wavebreaking term in the transfer equation has extracted a great deal of energy in this spectral region, thereby leaving a "hole" in the spectrum, as seen in Fig. 9.

Nonlinear Dispersion Relation

We have discussed how a surface current pattern perturbs the surface spectrum in a limited region of the ocean. We now turn our discussion toward how the surface spectrum affects a swell, i.e., a long wavelength gravity wave, as it passes through a restricted region of ocean. An analysis based on that presented for the spectral function yields the nonlinear dispersion relation

$$\omega_k = \omega_k^{(0)} - \int d^2L[4L^2\Gamma^{kL}_{kL}]\,\Psi(L) \tag{24}$$

for a spatially-uniform spectral function $\Psi(\boldsymbol{L})$, where $\omega_k^{(o)}[\equiv (gk)^{1/2}]$ is given by the linear dispersion relation for gravity waves and Γ^{kL}_{kL} is the coupling coefficient in Eq. (16). The normalization of the spectral density function for a continuous spectrum $\Psi(\boldsymbol{L})$ differs from that for a discrete spectrum $F(\boldsymbol{L})$.

We assume the ambient sea to be given by Phillips' saturated spectrum

$$\Psi(L) = (B/\pi)L^{-4} \tag{25}$$

where $B \approx 0.4\times10^{-2}$. Introducing the angle $\beta=\theta-\alpha$, where θ is the angle between the wavelength of interest $\boldsymbol{k}$ and the spectrum $\boldsymbol{L}$, and α is the angle between $\boldsymbol{L}$ and the wind, and integrating over angle in Eq.(24) yields the dispersion relation

$$\frac{\omega_k}{\omega_k^{(0)}} = 1 + \int_{u_1}^{u_2}\frac{du}{u^2}\,W(u,\beta);\quad u=k/L \tag{26}$$

Consider the case where a swell passes through a region of ocean which has a saturated spectrum at the higher wavenumbers. We may then ask what effect the ambient ocean has on the swell. In this case $L >> k$ for all L in the spectrum or $u << 1$ so that

$$W(u,\beta) \approx (Bu/2)(1+u^{1/2}\cos\beta)$$

which to first order in u is

$$W(u,\beta) \approx 2(B/4)u \tag{27}$$

Using Eq.(27) in Eq.(26), we obtain

$$\omega_k / \omega_k^{(0)} \approx 1 + \tfrac{1}{2} B \mathcal{L}n (u_2 / u_1) \tag{28}$$

where $u_2 = k/L_0$ and L_0 is the spectral peak which for a wind speed w is given by $L_0 = g/w^2$, and $u_1 = k/L_\gamma$ where $L_\gamma = (g/\gamma)^{1/2} = 370\ \mathrm{sec}^{-1}$ is the capillary wave cut-off wavenumber. Equation (28) may then be written as

$$\omega_k / \omega_k^{(0)} \approx 1 + \tfrac{1}{2} B \mathcal{L}n (L_\gamma / L_0)$$

Using the calculation of the mean square surface slope given by Philips, we obtain

$$\omega_k / \omega_k^{(0)} \approx 1 + \tfrac{1}{2} \langle (\nabla h)^2 \rangle \tag{29}$$

as the modification in the dispersion relation for the swell passing through a region of saturated sea. The frequency of the swell is increased by one half the mean-square slope of the region of ocean through which it passes. The change in swell frequency is reminiscent of the correction to the phase velocity of a Stokes Wave to second order, i.e., $C_{\mathrm{Stokes}} = \omega_k^{(0)} / k \ (1 + \tfrac{1}{2} k^2 a^2)$ where ka is the slope of the fundamental mode.

Conclusion

The eigenmode representation of the interaction equations provides one with a coherent theoretical structure with which to address problems of interest. The Spectral Function [Eq. (13)] originally considered by Wigner[18] allows one to implement the coupled mode rate equations in the construction of an equation for the spectrum of ocean waves. These two approaches to the interaction problem open a vast literature of calculational techniques which may be employed to further our understanding of the nonlinear interaction of ocean gravity waves.

References

[1]Lamb, H., *Hydrodynamics,* Chap. IX, 6th ed., Cambridge University Press, London, 1932.

[2]Lighthill, M. J., *Proceeding of the Royal Society of London,* Vol. A299, 1966, p. 28.

[3]Whitham, G. B., *Proceedings of the Royal Society of London,* Vol. A299, 1966, p. 2.

[4]West, B. J., Watson, K. M., and Thomson, J.A.L., "Mode Coupling of Ocean Wave Dynamics," *Physics of Fluids,* Vol. 17, 1974, p.1059; also entitled "Energy Spectra of the Ocean Surface: An Eigenmode Approach," RADC-TR-73-74, PD-72-030, Feb. 1973, Physical Dynamics, Inc., Berkeley, Calif.

[5]Benjamin, T. B. and Feir, J. E., *Journal of Fluid Mechanics,* Vol. 27, 1967, p 417.

[6]Lewis, J. E., Lake, B. M., and Ko, D.R.S., *Journal of Fluid Mechanics,* Vol. 63, 1974, p. 773.

[7]Hasselmann, K., *Journal of Fluid Mechanics,* Vol. 12, 1962, p. 481.

[8]Kinsman, B., *Wind Waves,* Prentice-Hall, Englewood Cliffs, N.J., 1965, p. 336.

[9]Watson, K. M. and West, B. J., "Spectral Evolution of the Ocean Surface," 1974, to be published in the *Journal of Fluid Mechanics;* also entitled "A Transport Equation Description of Non-Linear Ocean Surface Wave Interactions," RADC-TR-74-116, PD-73-048, Nov. 1973, Physical Dynamics, Inc., Berkeley, Calif.

[10]Thomson, J.A.L. and West, B. J., "A Spectral Transfer Model of Ocean Wave Spectra in the Presence of Non-Uniform Currents," to be published; also entitled: "A Spectral Transfer Model of Ocean Wave Spectra: I. Formulation," RADC-TR-73-192, PD-73-029, May 1973, Physical Dynamics, Inc., Berkeley, Calif.

[11]Watson, K.M., West, B.J., and Cohen, B.I., "Energy Spectra of the Ocean Surface: II. Interactions with Surface Currents, RADC-TR-74-15, PD-73-037, Oct. 1973, Physical Dynamics, Inc., Berkeley, Calif.

[12]Ref. 11, p.248.

[13]Zachariasen, F., "Internal Wave-Surface Wave Interaction Revisited," JASON Rept. 1972; available from NTIS AD-747332.

[14]Phillips, O.M., *The Dynamics of the Upper Ocean,* Cambridge University Press, London, 1968, p. 87.

[15]Longuet-Higgins, M. S. and Stewart, R. W., *Journal of Fluid Mechanics,* Vol. 10, 1961, p. 529.

[16]Pierson, W. J. and Stacy, R. A., "The Elevation, Slope and Curvature Spectra of a Wind Roughened Sea Surface," Contract NASI-10090, 1972, NASA; available from NTIS NASA-CR-2247.

[17]Thomson, J. A. L. and West, B. J., "Interaction of Non-Saturated Surface Gravity Waves with Internal Waves," 1974, submitted to the *Journal of Physical Oceanography;* also RADC-TR-72-280, PD-72-023, Oct. 1972, Physical Dynamics, Inc. Berkeley, Calif.

[18]Wigner, E. P., *Physical Review,* Vol. 40, 1932, p. 749.